Low-Resolution Molecular Structures of Isolated Functional Units from Arthropodan and Molluscan Hemocyanin

J. Günter Grossmann,* S. Abid Ali,†‡ Atiya Abbasi,† Zafar H. Zaidi,† Stanka Stoeva,‡ Wolfgang Voelter,‡ and S. Samar Hasnain*

*CCLRC Daresbury Laboratory, Warrington, Cheshire WA4 4AD, England; †HEJ Research Institute of Chemistry, University of Karachi, Karachi 75270, Pakistan; and ‡Physiologisch-Chemisches Institut, Universität Tübingen, 72076 Tübingen, Germany

ABSTRACT Synchrotron x-ray scattering measurements were performed on dilute solutions of the purified hemocyanin subunit (Bsin1) from scorpion (*Buthus sindicus*) and the N-terminal functional unit (Rta) from a marine snail (*Rapana thomasiana*). The model-independent approach based on spherical harmonics was applied to calculate the molecular envelopes directly from the scattering profiles. Their molecular shapes in solution could be restored at 2-nm resolution. We show that these units represent stable, globular building blocks of the two hemocyanin families and emphasize their conformational differences on a subunit level. Because no crystallographic or electron microscopy data are available for isolated functional units, this study provides for the first time structural information for isolated, monomeric functional subunits from both hemocyanin families. This has been made possible through the use of low protein concentrations (≤1 mg/ml). The observed structural differences may offer advantages in building very different overall molecular architectures of hemocyanin by the two phyla.

INTRODUCTION

Hemocyanins (Hcs) are high-molecular-mass, extracellular, copper-containing glycoproteins that perform the important function of oxygen transport in many species of arthropods and molluscs. Hemocyanins are not a homogeneous class of proteins; the sequence homology between arthropodan Hcs and their molluscan counterparts is rather low, 10% (Salvato and Beltramini, 1990); moreover, the molecular architectures, organization, size of the subunits, and metal contents are quite different in the two phyla (for a recent review see, e.g., van Holde and Miller, 1995).

Arthropod (crustacea and chelicerata) Hcs are hexameric (1 × 6-mers), and, depending on the species, one, two, four, six, or eight hexamers form the native Hc complex. The native Hc molecule of scorpion contains 24 subunits, arranged in four hexamers (4 × 6-mers), or two identical sets of dodecamers (2 × 12-mers). At alkaline pH and in the absence of divalent cations, the native molecule dissociates into eight immunologically distinct polypeptides, of which two are noncovalently linked heterodimers (Lamy et al., 1981). The single polypeptide has a molecular mass between 70 kDa and 75 kDa and is folded into three domains. The second or central domain contains one pair of copper atoms directly coordinated to the protein that forms the oxygen-binding site. The x-ray crystal structures of *Panulirus interruptus* (Pint) subunit a (crustacea) and *Limulus polyphemus* (Lpol) subunit II (chelicerata) Hcs have been resolved at 3.2 Å and 2.18 Å, respectively (Volbeda and Hol. 1989; Hazes et al., 1993).

Molluscan Hcs exist in the hemolymph as very large aggregates, assembled as 10-mers (Cephalopods and Chitons) or 20-mers (Bivalves and Gastropods). Hcs of many gastropods occur as even larger tubular structures, the so-called multidecamers. In electron micrographs decamers appear as cylinders with a three-tiered wall and a 5- or 10-fold symmetry of the collar in the central cavity (van Holde and Miller, 1995; Lamy et al., 1993; Miller et al., 1990). The monomer subunits with a molecular mass of 350–440 kDa are organized into a series of globular folded regions, clearly resolved under the electron microscope as a string of seven or eight beads of ~50 kDa, the so-called functional units or domains (van Holde and Miller, 1995). Each functional unit carries one binuclear copper site. There is a short flexible linker region consisting of 10–15 amino acid residues between each pair of functional units (Lang, 1988; Lang and van Holde, 1991), where specific cleavage can be achieved by limited proteolysis.

It is interesting to note that because of the size of native hemocyanin, it was one of the first metalloproteins to be investigated by the x-ray scattering method (Kratky, 1948) and has continued to attract much attention (Beltramini et al., 1996, 1999; Triolo et al., 1996; Decker et al., 1996). Here we have used this method to study the molecular conformation of single subunits in solution for the two classes by obtaining synchrotron x-ray scattering data for both an arthropodan (subunit Bsin1 from a scorpion) and a molluscan (N-terminal domain Rta from a marine snail) functional unit. (During the course of this work, a crystal structure of the dimeric C-terminal functional unit from *Octopus dofleini* at 2.3-Å resolution has been reported (Cuff et al., 1998), revealing a two-domain structure. Crystallographic coordinates have not yet been deposited with the

Received for publication 23 April 1999 and in final form 14 October 1999.

Address reprint requests to Prof. Samar Hasnain, CCLRC Daresbury Laboratory, Keckwick Lane, Warrington, Cheshire WA4 4AD, England. Tel.: +44-1925-603273; Fax: +44-1925-603748; E-mail: s.hasnain@dl.ac.uk.

0006-3495/00/02/977/05 $2.00

PDB.) The crystallographic structures of arthropodan Hcs (Pint subunit a and Lpol subunit II) have been of the hexameric assembly. It is also of interest to know if the structure of an isolated single functional subunit is retained when it is outside the multimeric assembly. Recent advances in x-ray scattering data analysis, coupled with synchrotron radiation scattering instruments that enable data collection to reasonably high angles (~3–5°), have made this an ideal technique for providing low-resolution structural information on proteins or their complexes in solution. The availability of intense, well-collimated x-ray beams from synchrotron radiation sources allows the recording of statistically significant scattering data over a wide angular range (Grossmann and Hasnain, 1997), even at low protein concentrations ($\leq$ 1 mg/ml).

MATERIALS AND METHODS

Purification and concentration of hemocyanin samples

Scorpions (*Buthus sindicus,* family Buthidea) were collected from the province of Sindh, Pakistan. Hemolymph was collected by direct heart puncture from adult scorpions and centrifuged at 5000 rpm for 5 min to remove cellular fragments. Hemocyanin was sedimented in an ultracentrifuge (Hitachi model 85S) at 50,000 rpm for 4 h at 5°C, and the blue pellet was resuspended in 50 mM Tris/HCl buffer (pH 7.5) containing 10 mM $CaCl_2$. Purification of scorpion hemocyanin subunits Bsin1 was performed as described previously (Ali et al., 1995). The oxygenated state of purified Bsin1 was prepared by dialysis against 50 mM Tris/HCl buffer (pH 7.5), 10 mM EDTA (instead of $CaCl_2$), to prevent self-aggregation of polypeptide subunits, at room temperature (~20°C) for 24 h. Scattering measurements were performed at protein concentrations of 1 and 0.5 mg/ml.

Living marine snails (*Rapana thomasiana* grosse, order Monotocardia, family Thaididae) were caught near the northern Bulgarian coast of the Black Sea and stored in seawater before the collection of the hemolymph. Isolation of the hemocyanin and its structural subunits (RHSS1 and RHSS2) was performed as described previously (Boteva et al., 1991; Idakieva et al., 1993). Purification of the N-terminal domain (Rta) from the 450-kDa subunit RHSS2 was reported recently (Idakieva et al., 1995; Stoeva et al., 1997). The oxygenated native hemocyanin was prepared by dialysis against 50 mM Tris/HCl buffer (pH 8.2) containing 5 mM EDTA, at room temperature (~20°C) for 24 h. For the scattering measurements protein concentrations of 0.5, 0.7, and 1 mg/ml were used.

Synchrotron x-ray scattering experiments

X-ray scattering experiments were performed on beamline 2.1 at the Synchrotron Radiation Source (Daresbury, England) (Towns-Andrews et al., 1989) at an electron energy of 2 GeV and with beam currents between 180 mA and 250 mA. The sample-to-detector distance was 2.8 m (2.3 m) for Bsin1 (Rta), which allowed data collection between 0.05 $nm^{-1} \leq s \leq$ 0.38 nm^{-1} (0.07 $nm^{-1} \leq s \leq$ 0.45 nm^{-1}), where $s = (2 \sin \Theta)/\lambda$ (2Θ is the scattering angle and λ is the x-ray wavelength of 0.15 nm), on a position-sensitive quadrant multiwire proportional counter with an associated data acquisition system (Lewis et al., 1988). The scattering pattern from an oriented specimen of wet rat tail collagen was used to calibrate the detector for each camera length. Parallel plate ionization chambers placed before and after the sample cell recorded incident and transmitted intensities. Samples were measured at room temperature (~21°C) in a brass cell containing a Teflon ring sandwiched by two mica windows, which defines the sample volume of 120 μl and a path length of 0.25 cm. To minimize systematic errors, each data set consisted of buffer followed by protein data collection. The experimental data were recorded in frames of 30 s, allowing on-line checks for changes in the scattering profiles, and corrected for background scattering (subtraction of the scattering from the camera and a cell filled with buffer), sample transmission and concentration, and positional nonlinearities of the detector. The total data collection time for each sample was 30 min.

Scattering data analysis

Off-line data reduction was done with the OTOKO software package (Boulin et al., 1986). The individual scattering curves were analyzed using the indirect transform method, as implemented in the programme package GNOM (Semenyuk and Svergun, 1991), which makes use of the entire data range. This method is more reliable than the use of a restricted portion of data, as in the case of the Guinier approximation for the calculation of the radius of gyration, R_g (Guinier, 1939). The *ab initio* determination of a molecular shape directly from the scattering profile alone was performed using a model-independent procedure that also exploits the information inherent in the wider-angle scattering data. This procedure, based on the multipole expansion method using spherical harmonics, has been described elsewhere in greater detail (Svergun et al., 1997; Grossmann and Hasnain, 1997; Grossmann et al., 1998). Assuming the scattering is caused by a globular, homogeneous molecule, one can define its molecular shape by the angular envelope function $F(\theta, \varphi)$ such that the particle density $\rho(r)$ is unity inside the molecular boundary and vanishes elsewhere. $F(\theta, \varphi)$ can be expanded into a series of spherical harmonics $Y_{lm}(\theta, \varphi)$ according to (Stuhrmann, 1970)

$$F(\theta, \varphi) = R_O \sum_{l=0}^{L} \sum_{m=-l}^{l} f_{lm} Y_{lm}(\theta, \varphi)$$

where R_o is a scale factor and f_m is complex multipole coefficients. The resolution is determined by the maximum order of harmonics, i.e., the highest value of L. It is a nonlinear equations system that interrelates the f_{lm} coefficients with coefficients of the power series describing the experimental scattering curve. Svergun and Stuhrmann (1991) developed a reliable nonlinear optimization procedure to evaluate the multipole coefficients by minimizing a residual R between calculated and experimental curves. A detailed discription of the minimization procedure can be found in Svergun et al. (1996). Because no molecular symmetry can be assumed for the two proteins, the available experimental data range and the number of free parameters [i.e., $(L + 1)^2$-6] limit the number of coefficients for a unique shape description up to the multipole order of $L = 3$ (which corresponds to 10 independent parameters; Svergun et al., 1996). However, because there is no significant shape difference shown by increasing the multipole calculation to the order of $L = 4$ (i.e., the uniqueness of the molecular envelope in going from $L = 3$ to $L = 4$ is preserved), we present here the results for the shape restoration with $L = 4$. This multipole order is characterized by 25 coefficients, of which 19 are independent. The analysis of the flm coefficients for the shape model at $L = 4$ shows that five of the 25 parameters are negligibly small (<0.02), which emphasizes once more that there is no significant shape difference between $L = 3$ and $L = 4$. More details concerning treatment of scattering data are given elsewhere (Grossmann et al., 1998).

RESULTS AND DISCUSSION

A comparison of scattering profiles and intraparticle distance distributions for both hemocyanin subunits is presented in Fig. 1 *A*. To minimize self-aggregation of Hc

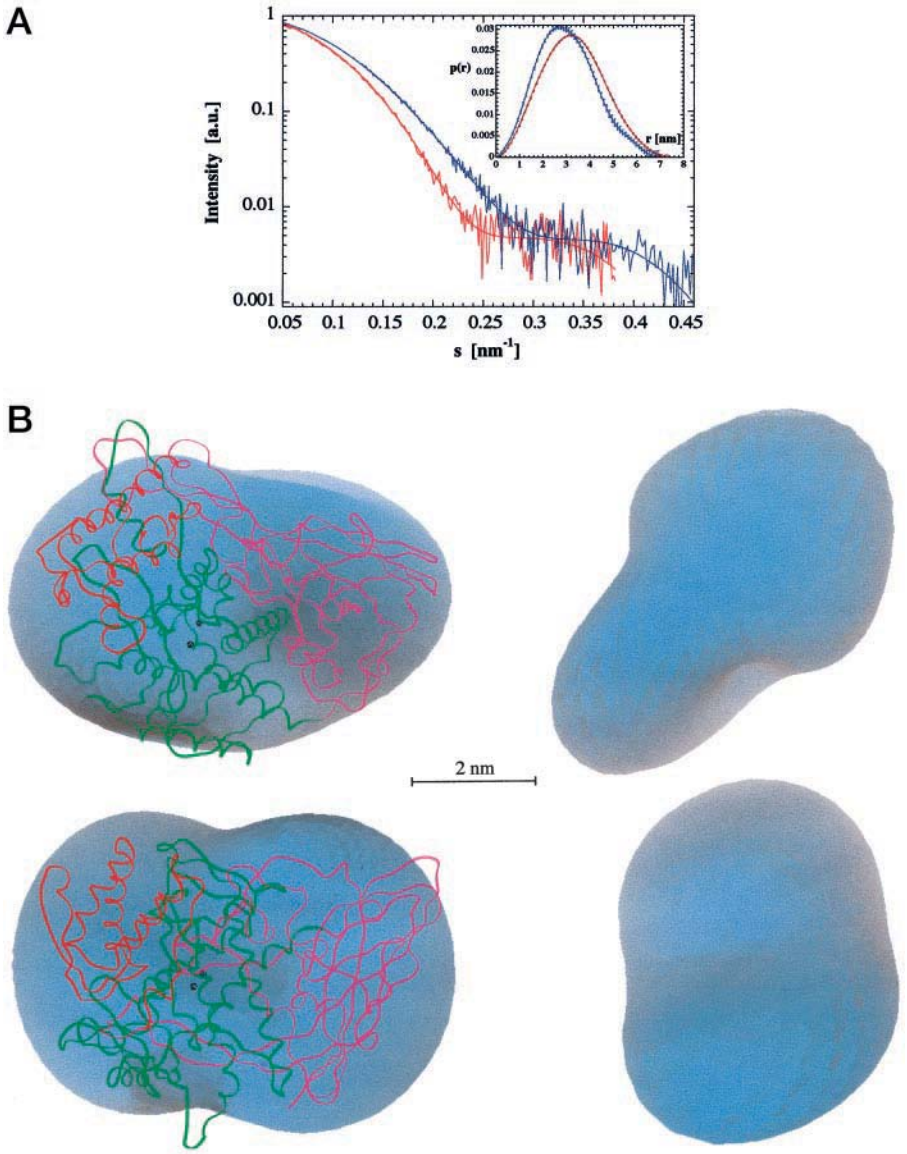

FIGURE 1 (*A*) Scattering profiles and distance distribution functions (*inset*) of the functional subunit Bsin1 from scorpion (*red*) and of the purified N-terminal domain Rta from marine snail (*blue*) in the oxygenated state. The smooth curves represent the scattering curves resulting from the restored shapes up to the multipole order $L = 4$. (*B*) Two orientations of the molecular envelopes for Bsin1 (*left-hand pictures*) and Rta (*right-hand pictures*) deduced from the scattering profiles shown in *A*. Top and bottom pictures for Bsin1 are related by a 90° rotation around the horizontal axis. The backbone ribbon of the functional subunit II from *Limulus polyphemus* in the oxygenated state is superimposed (the three domains are depicted in different colors). PDB code, 1nol (Bernstein et al., 1977). The shape representations for Rta correspond approximately to the two orientations of the upper monomer in the molecular dimer of *Octopus dofleini* subunit g, given in figure 8 of Cuff et al. (1998).

subunits, only low concentrations have been used in both cases (≤1 mg/ml). Despite this restriction, a good signal-to-noise ratio was achieved, even in the outermost scattering regime, which allowed a reliable data interpretation. A summary of geometrical parameters is provided in Table 1. The molecular envelopes were restored *ab initio* at a resolution of 2 nm, as described under Materials and Methods. The solutions giving the best fit to the experimental scattering profile for both Bsin1 (with final residual $R = 1.3\%$) and Rta ($R = 1.1\%$), obtained with spherical harmonics terms up to $L = 4$, are included in Fig. 1 *A*. The corresponding molecular envelopes for each Hc functional unit are shown in two orientations in Fig. 1 *B*.

The crystal structure from an arthropodan subunit *(Limulus polyphemus* subunit II (Lpol2)) is superimposed on the shape of Bsin1 deduced from the solution scattering data in Fig. 1 *B*. The evaluation of the overall conformation of Bsin1 was feasible, not only in view of the availability of an atomic structure of an arthropod Hc subunit in the oxygenated state, but also because of the close sequence homology

TABLE 1 Geometrical parameters of hemocyanin functional units from arthropodan (Bsin1) and molluscan (Rta) sources extracted from solution x-ray scattering data

	R_g (nm)	D_{max} (nm)	Volume (nm^3)
Bsin1	2.50 ± 0.04*	7.2 ± 0.3	114 ± 5
Rta	2.30 ± 0.04	6.9 ± 0.3	81 ± 3

*For comparison the calculated R_g values for the solvated arthropod Hc subunit structures of oxy-Lpol2 (PDB code 1nol), deoxy-Lpol2 (1lla), and deoxy-Pint1 (1hc1) are 2.50 nm, 2.49 nm, and 2.60 nm, respectively. The solvated Hc subunit structures were evaluated with the program CRYSOL (Svergun et al., 1995), which takes the scattering from a hydration shell into account. The value of R_g for Bsin1 is in excellent agreement with values reported recently by Beltramini et al. (1999).

between Lpol2 and Bsin1 (Ali et al., 1995; Ali, 1997). The molecular shape for Bsin1 agrees well with the crystal structure of oxy-Lpol2 (Magnus et al., 1994), as can be seen from Fig. 1 *B* (*left-hand side*). So far more than 60% of the amino acid sequence of Bsin1 is known (Ali, 1997), including the fragments that have been identified for Lpol2 in providing ligands for the binuclear copper active site and putative calcium and chloride binding site. This partial primary structure of Bsin1 shows a high sequence homology with the immunologically related subunit from horseshoe crab, *L. polyphemus* subunit II (57%), and spider, *E. californicum* chain a (53%). Structurally important residues delineated for Lpol2 around the active site copper atoms, the calcium binding site, and the presumed oxygen entrance pathway are strictly conserved in Bsin1. Sequence variation was found around the chloride-binding site (Ali, 1997). A chloride ion has been proposed to play an important part in inhibiting the T (low affinity) to R (high affinity) transition; thus differences in the two crystal structures of deoxy-Hcs have been suggested to arise from the Cl^- binding in the *L. polyphemus* subunit II structure (Magnus et al., 1994). Our studies were performed on the oxygenated state, and the samples contained Tris/HCl in the buffer. Although solution x-ray scattering is a low-resolution technique, it is capable of detecting changes in the arrangement of subunits or domains. Our scattering results for Bsin1 are clearly in better agreement with the "T-state" (oxy-Lpol2) rather than with what has been suggested to be the R-state conformation (characterized by the crystal structure of deoxygenated *P. interruptus* hemocyanin; Volbeda and Hol, 1989). This is emphasized by the radii of gyration calculated from the solvated crystal structures of oxy/deoxy-Lpol2 and deoxy-Pint1 (see also annotations to Table 1). Deoxy-Pint1 reveals a notably larger radius of gyration, i.e., a less compact conformation compared to oxy/deoxy-Lpol2 (owing to a major difference in the orientation of the first domain, which can be described as a 7.5° rigid-body motion with respect to the other two domains; Hazes et al., 1993). However, we also note that certain subunits (e.g., the hemocyanin subunit 3A from the scorpion species *Androctonus australis*) have been found to play an important role in stabilizing a conformation of low oxygen affinity (Lamy et al., 1980).

Unlike the bean-shaped molecular conformation of Bsin1, the overall shape of Rta displays a globular core domain with a neck-like extension (Fig. 1 *B, right-hand side*). This is reminiscent of the crystal structure of the dimeric C-terminal functional unit from *Octopus dofleini* (Odg), which was published during the course of this study (Cuff et al., 1998). Because of the nonavailability of the crystal structure coordinates of this molluscan functional unit Odg, the molecular shape of the Rta monomer is arranged in analogy to the upper monomer shown in figure 8 of Cuff et al. (1998), which gives two orientations of the molecular dimer of Odg. We note here that at the low concentrations used for our x-ray scattering experiments, only the isolated subunits could be detected in solution. One may speculate whether this finding is related to the location of functional units within a subunit of molluscan hemocyanin (Rta represents the N-terminal unit, whereas Odg is located at the C-terminal end). In any case, a sequence homology of ~50% between Rta and Odg (Stoeva et al., 1997) and their very similar overall conformations indicate the close structural resemblance of individual molluscan functional units, as well as those belonging to different members of the phyla. We note that the putative carbohydrate attachment sites differ in Rta and Odg. Odg possesses only one glycosylation site, which has clearly been identified in the crystal structure as being attached to the core domain and extending along the smaller second domain (Cuff et al., 1998; Miller et al., 1998). In contrast, the two potential glycosylation sites in Rta, Asn^{27} and Asn^{250} (Stoeva et al., 1997), both belong to the core domain and are located at the opposite end with respect to the smaller domain. This is reflected in the molecular shape of Rta, which emphasizes a globular core with a neck-like extension due to the smaller domain.

In conclusion, this study provides for the first time structural details of hemocyanins represented by their monomeric functional units in solution, which has been made possible by the use of low protein concentrations ($\leq$1 mg/ml). The *ab initio* low-resolution models deduced from synchrotron x-ray solution scattering profiles agree well with the respective counterparts examined in the solid state. Moreover, because there is no crystallographic or electron microscopic data available for strictly monomeric functional units, our study confirms that these hemocyanin building blocks represent stable structures in solution. The results clearly demonstrate that the two classes of hemocyanin differ at the level of their subunit structures. These differences have also been reported in crystallographic studies of different members of the two families. The structural differences observed for the two families may offer particular advantages in forming the unique multimeric hemocyanin assemblies (i.e., hexameric assemblies for the arthropods and decamers for the molluscan hemocyanins). Future x-ray scattering studies should be directed at the larger assemblies of both classes of hemocyanin.

We thank the Council for the Central Laboratory of the Research Councils and the Biotechnology and Biological Sciences Research Council for the provision of facilities at the Daresbury Laboratory. We are particularly grateful to Dr. D. I. Svergun for making available the spherical harmonics calculation program package to us.

This work was initiated when SAA was a visiting scientist at Daresbury Laboratory. SAA also acknowledges the Deutscher Akademischer Austauschdienst (DAAD) for partial support of this work.

REFERENCES

Ali, S. A. 1997. Primary structure of hemocyanin from scorpion (*Buthus sindicus*). Ph.D. thesis. University of Karachi, Karachi, Pakistan.

Ali, S. A., Z. H. Zaidi, and A. Abbasi. 1995. Oxygen transport proteins. I. Structure and organisation of hemocyanin from scorpion (*B. sindicus*). *Comp. Biochem. Physiol.* 112A:225–232.

Beltramini, M., E. Borghi, P. Di Muro, A. La Monaca, B. Salvato, and C. Santini. 1996. Functional SAXS study of hemocyanin dioxygen-carrier protein. *J. Mol. Struct.* 383:237–240.

Beltramini, M., P. Di Muro, R. Favilla, A. La Monaca, P. Mariani, A. L. Sabatucci, B. Salvato, and P. L. Solari. 1999. SAXS investigation on the temperature dependence of the conformation of *Carcinus aestuarii* 5S hemocyanin subunit. *J. Mol. Struct.* 475:73–82.

Bernstein, F. C., T. F. Koetzle, G. J. B. Williams, F. M. Meyer, Jr., M. D. Brice, J. R. Rodgers, O. Kennard, T. Shimanouchi, and M. Tasumi. 1977. The Protein Data Bank: a computer-based archival file for macromolecular structures. *J. Mol. Biol.* 112:535–542.

Boteva, R., S. Severov, N. Genov, M. Beltramini, B. Filiph, F. Ricchelli, L. Tallandini, M. M. Pallhuber, G. Tognion, and B. Salvato. 1991. Biochemical and functional characterization of *Rapana thomasiana* hemocyanin. *Comp. Biochem. Physiol.* 100B:493–501.

Boulin, C., R. Kempf, M. H. J. Koch, and S. M. McLaughlin. 1986. Data appraisal, evaluation and display for synchrotron radiation experiments: hardware and software. *Nucl. Instrum. Methods Phys. Res.* A249: 399–407.

Cuff, M. E., K. I. Miller, K. E. van Holde, and W. A. Hendrickson. 1998. Crystal structure of a functional unit from octopus hemocyanin. *J. Mol. Biol.* 278:855–870.

Decker, H., H. Hartmann, R. Sterner, E. Schwarz, and I. Pilz. 1996. Small-angle x-ray scattering reveals differences between the quaternary structures of oxygenated and deoxygenated tarantula hemocyanin. *FEBS Lett.* 393:226–230.

Grossmann, J. G., J. B. Crawley, R. W. Strange, K. J. Patel, L. M. Murphy, M. Neu, R. W. Evans, and S. S. Hasnain. 1998. The nature of ligand induced conformational change in transferrin in solution: an investigation using x-ray scattering, XAFS and site-directed mutants. *J. Mol. Biol.* 279:461–472.

Grossmann, J. G., and S. S. Hasnain. 1997. X-ray scattering studies of metalloproteins in solution: a quantitative approach for studing molecular conformations. *J. Appl. Crystallogr.* 30:770–775.

Guinier, A. 1939. La diffraction des rayons X aux très petits angles, application à l'étude de phénomènes ultramicroscopiques. *Ann. Physique.* 12:161–237.

Hazes, B., K. A. Magnus, C. Bonaventura, J. Bonaventura, Z. Dauter, K. H. Kalk, and W. G. J. Hol. 1993. Crystal structure of deoxygenated *Limulus polyphemus* subunit II hemocyanin at 2.18 Å resolution: clues for a mechanism for allosteric regulation. *Protein Sci.* 2:597–619.

Idakieva, K., S. Severov, I. Svendsen, N. Genov, S. Stoeva, M. Beltramini, G. Tognon, P. Di Muro, and B. Salvato. 1993. Structural properties of *Rapana thomasiana grosse* hemocyanin: isolation, characterization and N-terminal amino acid sequence of two different dissociation products. *Comp. Biochem. Physiol.* 106B:53–59.

Idakieva, K., S. Stoeva, W. Voelter, and N. Genov. 1995. Functional unit of *Rapana thomasiana* (grosse) (marine snail, gastropod) hemocyanin. *Comp. Biochem. Physiol.* 112B:599–606.

Kratky, O. 1948. Low-angle scattering in polymers. *J. Polym. Sci.* 3:195–215.

Lamy, J., M. M. C. Bijiholt, P. Y. Sizaret, J. Lamy, and E. F. J. Van Bruggen. 1981. Quaternary structure of scorpion (*Androctonus australis*). Localization of subunits with immunological methods and electron microscopy. *Biochemistry.* 20:1849–1856.

Lamy, J., C. Gielens, O. Lambert, J. C. Taveau, G. Motta, P. Loncke, and N. Degeest. 1993. Further approaches to the quaternary structure of octopus hemocyanin—a model based on immunoelectron microscopy and image processing. *Arch. Biochem. Biophys.* 305:17–29.

Lamy, J., J. Lamy, J. Bonaventura, and C. Bonaventura. 1980. Structure function and assembly in the hemocyanin system of the scorpion *Androctonus australis. Biochemistry.* 19:3033–3039.

Lang, W. H. 1988. cDNA cloning of the *Octopus dofleini* hemocyanin—sequence of the carboxyl-terminal domain. *Biochemistry.* 27: 7276–7282.

Lang, W. H., and K. E. van Holde. 1991. Cloning and sequencing of *Octopus dofleini* hemocyanin cDNA derived sequences of functional units Ode and Odf. *Proc. Natl. Acad. Sci. USA.* 88:244–248.

Lewis, R., I. Sumner, A. Berry, J. Bordas, A. Gabriel, G. Mant, G. Parker, K. Roberts, and J. Worgan. 1988. Multiwire x-ray detector system at the Daresbury SRS. *Nucl. Instrum. Methods Phys. Res.* A273:773–777.

Magnus, K. A., B. Hazes, H. Ton-That, C. Bonaventura, J. Bonaventura, and W. G. J. Hol. 1994. Crystallographic analysis of oxygenated and deoxygenated states of arthropod hemocyanin shows unusual differences. *Proteins Struct. Funct. Genet.* 19:302–309.

Miller, K. I., M. E. Cuff, W. F. Lang, P. Varga-Weisz, K. G. Field, and K. E. van Holde. 1998. Sequences of the *Octopus dofleini* hemocyanin subunit: structural and evolutionary implications. *J. Mol. Biol.* 278: 827–842.

Miller, K. I., E. Schabtach, and K. E. van Holde. 1990. Arrangement of subunits and domains within the *Octopus dofleini* hemocyanin molecule. *Proc. Natl. Acad. Sci. USA.* 87:1496–1500.

Salvato, B., and M. Beltramini. 1990. Hemocyanins: molecular architecture, structure and reactivity of the binuclear copper active site. *Life Chem. Rep.* 8:1–47.

Semenyuk, A. V., and D. I. Svergun. 1991. GNOM—a program package for small-angle scattering data processing. *J. Appl. Crystallogr.* 24: 537–540.

Stoeva, S., K. Idakieva, N. Genov, and W. Voelter. 1997. Complete amino acid sequence of dioxygen-binding functional unit of the *Rapana thomasiana* hemocyanin. *Biochem. Biophys. Res. Commun.* 238:403–410.

Stuhrmann, H. B. 1970. Interpretation of small-angle scattering functions of dilute solutions and gases. A representation of the structures related to a one-particle-scattering function. *Acta Crystallogr.* A26:297–306.

Svergun, D., C. Barberato, and M. H. J. Koch. 1995. CRYSOL—a program to evaluate x-ray solution scattering of biological macromolecules from atomic coordinates. *J. Appl. Crystallogr.* 28:768–773.

Svergun, D. I., and H. B. Stuhrmann. 1991. New developments in direct shape determination from small-angle scattering. 1. Theory and model calculations. *Acta Crystallogr.* A47:736–744.

Svergun, D. I., V. V. Volkov, M. B. Kozin, and H. B. Stuhrmann. 1996. New developments in direct shape determination from small-angle sctering. 2. Uniqueness. *Acta Crystallogr.* A52:419–426.

Svergun, D. I., V. V. Volkov, M. B. Kozin, H. B. Stuhrmann, C. Barberato, and M. H. J. Koch. 1997. Shape determination from solution scattering of biopolymers. *J. Appl. Crystallogr.* 30:798–802.

Towns-Andrews, E., A. Berry, J. Bordas, G. R. Mant, P. K. Murray, K. Roberts, I. Sumner, J. S. Worgan, and R. Lewis. 1989. Time-resolved x-ray diffraction station: x-ray optics, detectors, and data acquisition. *Rev. Sci. Instrum.* 60:2346–2349.

Triolo, F., V. Graziano, and R. H. Heenan. 1996. Small angle neutron scattering study of the quaternary structure of hemocyanin of *Rapana thomasiana. J. Mol. Struct.* 383:249–254.

van Holde, K. E., and K. I. Miller. 1995. Hemocyanins. *Adv. Protein Chem.* 47:1–81.

Volbeda, A., and W. G. J. Hol. 1989. Crystal structure of hexameric haemocyanin from *Panulirus interruptus* refined at 3.2 Å resolution. *J. Mol. Biol.* 209:249–279.